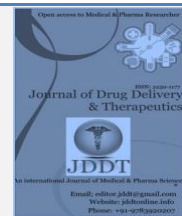
Available online on 15.11.2023 at <http://jddtonline.info>

# Journal of Drug Delivery and Therapeutics

Open Access to Pharmaceutical and Medical Research

Copyright © 2023 The Author(s). This is an open-access article distributed under the terms of the CC BY-NC 4.0 which permits unrestricted use, distribution, and reproduction in any medium for non-commercial use provided the original author and source are credited



Open Access Full Text Article



Check for updates

Research Article

## Nanoencapsulation of *Rosmarinus officinalis* essential oil into Chitosan crosslinked to Tripolyphosphate nanoparticles and Alginate/Chitosan nanoparticles: Formulation, characterization, in vitro release study, and in vivo evaluation

HELLALI Djafer Hamza\*<sup>1</sup>, AYACHI Nabila

Galenic Pharmacy Laboratory, Pharmacy Department, Medicine Faculty, Blida 1 DAHLEB Saad University, 09000. Blida, Algeria

### Article Info:



#### Article History:

Received 26 Aug 2023  
Reviewed 02 Oct 2023  
Accepted 19 Oct 2023  
Published 15 Nov 2023

#### Cite this article as:

Hellali DH, Nabila A, Nanoencapsulation of *Rosmarinus officinalis* essential oil into Chitosan crosslinked to Tripolyphosphate nanoparticles and Alginate/Chitosan nanoparticles: Formulation, characterization, in vitro release study, and in vivo evaluation, *Journal of Drug Delivery and Therapeutics*. 2023; 13(11):45-55

DOI: <http://dx.doi.org/10.22270/jddt.v13i11.6270>

#### \*Address for Correspondence:

HELLALI Djafer Hamza, Galenic Pharmacy Laboratory, Pharmacy Department, Medicine Faculty, Blida 1 DAHLEB Saad University, 09000. Blida, Algeria

### Abstract

This study delves into the intricate realm of nanoencapsulation, focusing on the application of chitosan crosslinked to TPP and alginate/chitosan-based nanoparticles to encapsulate *Rosmarinus officinalis* essential oil. The core objective was to unravel the potential pharmacological merits and controlled release dynamics underpinning this novel encapsulation technique. The experimental results painted a compelling portrait of rosemary oil, showcasing its multifaceted efficacy as an antibacterial, antifungal, and antioxidant agent. In the realm of nanotechnology, we were able to formulate nanoparticles under 100 nm, demonstrating exceptional stability. A pivotal aspect of this research revolved around encapsulation efficiency, determined via UV-vis spectroscopy. The results proved staggering, illustrating an encapsulation rate surpassing the 98% benchmark, ensuring minimal essential oil wastage. In vitro assays illuminated the controlled, sustained release attributes of the encapsulated essential oil, thereby further substantiating the potential of this encapsulation approach. FTIR analysis provided insights into the intricate interactions transpiring within these nanoparticles. Venturing into living organisms, our comprehensive in vivo assessments confirmed the significant analgesic activity of our nanoparticles encapsulating rosemary essential oil. This revelation opens exciting prospects for therapeutic applications. Microscopic observations into the SEM solidified the presence and even distribution of these nanoparticles. These compelling findings chart new avenues for the development of more potent, precisely targeted pharmaceutical interventions.

**Keywords:** Rosemary essential oil, chitosan, sodium alginate, polymeric nanoparticles, nanoencapsulation

## INTRODUCTION

In the sphere of pharmaceutical and biotechnological advancements, rigorous research and cutting-edge technologies have ushered in a transformative era in drug delivery and encapsulation systems. This narrative unfolds against the backdrop of essential elements such as polymers, nanoencapsulation, and essential oils, which are foundational to the future of pharmaceutical science.

Polymers, exemplified by chitosan and sodium alginate, occupy a central role in the design of advanced drug delivery systems. Chitosan, a biopolymer derived from chitin, possesses a unique blend of biocompatibility and biodegradability. Its cationic nature renders it an ideal candidate for complex pharmaceutical formulations, enabling controlled drug release and enhancing therapeutic efficacy<sup>1</sup>. On the other hand, sodium alginate, a polysaccharide sourced from brown seaweed, complements these attributes by forming gel-like matrices<sup>2</sup>. The synergy between these oppositely charged polymers establishes a

versatile platform for pharmaceutical innovations. Nanoencapsulation, an intricate science conducted at the nanoscale, represents a pinnacle achievement in our pursuit of advanced drug delivery. By encapsulating therapeutic agents within nanoparticles, this methodology unlocks a myriad of possibilities. These nanocarriers, meticulously engineered and controlled, offer the potential to revolutionize pharmaceuticals. They empower precise modulation of drug release profiles, elevating bioavailability and enabling targeted delivery<sup>3</sup>. At this scale, the science of encapsulation provides solutions to persistent challenges such as drug stability, solubility, and controlled release, propelling the pharmaceutical industry into a new era of possibilities. At the heart of our exploration lies rosemary essential oil (REO), a botanical repository celebrated for its multifaceted activities<sup>4</sup>. From its distinguished antibacterial and antifungal attributes to its robust antioxidant capacity, REO embodies therapeutic versatility<sup>5</sup>. However, despite its myriad advantages, REO poses challenges concerning stability, solubility, and controlled release of its active

components<sup>6</sup>. However, the complete realization of its potential within the intricate domain of drug delivery demands a systematic approach—one that integrates its biological activities with the precision of nanoencapsulation.

Drug delivery, a cornerstone of pharmaceutical science, aims to optimize the journey of therapeutic agents within the human body. It is a discipline dedicated to maximizing efficacy while minimizing undesirable side effects. The encapsulation of REO within nanoparticles signifies a paradigm shift, granting access to a realm of heightened stability, controlled release, and the harnessing of therapeutic potential<sup>7</sup>.

In light of these considerations, the primary objective of this study is to process into the formulation of chitosan crosslinked with sodium tripolyphosphate (TPP) and chitosan/alginate nanoparticles encapsulating REO to enhance its stability. This encapsulation approach seeks to address the intrinsic limitations of REO, expanding its potential utility in the realm of pharmaceuticals. In doing so, we aspire to illuminate novel pathways in pharmaceutical research, offering innovative solutions for drug encapsulation and delivery.

## MATERIALS AND METHODS

### Raw materials

Chitosan and Sodium alginate, sourced from Sigma–Aldrich Chemical Co. Ltd. (St. Louis, MO, USA). Essential oil of *Rosmarinus officinalis* (region of Tipaza, specifically from the mountains of Djebell el Nador) was purchased from a local herbal store. Carrageenan was provided from Sigma–Aldrich Chemical Co. Ltd. (St. Louis, MO, USA), and tripolyphosphate sodium from Prayon (Belgium). Calcium carbonate and all solvents used were of analytical grade, ensuring the purity of our experimental results. Deionized distilled water was utilized throughout the experiments.

### Maintenance of cell culture

To assess the antimicrobial properties of our rosemary essential oil, we utilized a diverse panel of bacterial and fungal strains. Among the tested microorganisms, two Gram-positive bacteria were included: *Staphylococcus aureus* ATCC 25923 and *Enterococcus faecalis* ATCC 29212. Additionally, five Gram-negative bacteria were investigated: *Escherichia coli* ATCC 25922, *Klebsiella pneumoniae*, *Pseudomonas aeruginosa* ATCC 27853, *Serratia marcescens*, and *Salmonella enterica*. Furthermore, our study encompassed three *Candida* pathogens: *Candida albicans*, *Candida kefyr*, and *Candida glabrata*. It should be noted that except for the ATCC strains, all other strains were isolated directly from patients.

These microbial strains were sourced from the Microbiology and Parasitology laboratory of the hospital establishment specializing in organ and tissue transplantation of Blida, Algeria. Bacterial strains were re-isolated on nutrient agar medium, while the Fungi strains were re-isolated on Sabouraud chloramphenicol medium to maintain their viability and purity during the experimental procedure.

### Experimental Animals

In this study, either sex of NMRI mice with a mean weight of  $23 \pm 2$  g were utilized as the experimental model. These mice were procured from the Institute of Pasteur of Algeria and served as an essential component of our research. The animals were housed in groups of 3–6 per cage, ensuring a social environment, and were provided with unrestricted access to both food and

water throughout the study. To maintain the welfare of the animals and minimize potential confounding factors, they were kept under standard laboratory conditions. Specifically, the mice were housed in appropriate cages designed to replicate a natural daytime environment. These conditions were meticulously maintained throughout the entire experiment to uphold the well-being of the animals and to guarantee the consistency and reliability of the study's outcomes.

### Antimicrobial activity of rosemary essential oil

#### a. Determination of antibacterial activity

The antimicrobial effectiveness of rosemary essential oil was assessed using both the aromatogram method and by establishing its Minimum Inhibitory Concentration (MIC).

The aromatogram is a technique for testing the antibacterial activity of essential oils. It was conducted using the agar well diffusion method and the disk diffusion method<sup>8, 9</sup>. The preparations of bacterial suspensions were standardized to an optical density of 0.5 to 0.6 McFarland using a densimeter. A precise volume of 50 microliters of the pure essential oil was meticulously impregnated onto sterile filter paper disks that are aseptically placed onto the surface of Mueller-Hinton agar medium which had been previously inoculated with the standardized bacterial suspensions. Additionally, as a part of the assessment, 100 microliters of the pure essential oil were introduced into the well created within the same Mueller-Hinton agar medium. A gentamicin 10 mg disc served as a positive control. After incubating at 37°C for 24 hours, results were interpreted by measuring the zone of bacterial growth inhibition formed. Each plate was inspected to evaluate the presence of zones where growth was inhibited, the measurement of these zones diameter was conducted in millimeters.

#### *Determination of minimum inhibitory concentration (MIC) for Antibacterial activity*

Subsequently, we determined the Minimum Inhibitory Concentration (MIC) of *Rosmarinus officinalis* essential oil against bacterial strains using the microdilution method with 96-well microplates as described by Aouni and al.<sup>10</sup>. The MIC represented the lowest essential oil concentration inhibiting bacterial growth<sup>11</sup>. Dilutions of REO were prepared in Brain Heart Infusion Broth (BHIB) and 1% Tween 80. Each well received 10  $\mu$ l of the essential oil dilution and 90  $\mu$ l of a bacterial suspension (approximately  $10^6$  CFU/ml) in order to obtain the concentrations of essential oil ranging from 4  $\mu$ g/ml to 0.008  $\mu$ g/ml. After incubation at 37°C for 24 hours, MICs were determined by assessing the turbidity of the bacterial suspension in the wells. Clear and transparent wells indicated bacterial inhibition, while cloudy wells suggested continued growth.

#### b. Determination of antifungal activity

To assess the antifungal properties of REO, we adapted the methods used for antibacterial testing, with minor adjustments. For fungal cultures, we used Sabouraud agar medium supplemented with chloramphenicol. The fungal suspensions were standardized to an optical density of approximately

2 McFarland. The results were obtained after incubation of the microplate at temperatures ranging from 25°C to 37°C for 24 to 48 hours, depending on the specific candida strain by measuring the diameter of the fungal growth inhibition zones around the wells and disk containing REO, that are present on the surface of the Sabouraud chloramphenicol medium.

### Determination of minimum inhibitory concentration (MIC) for Antifungal activity:

The same microdilution method with 96-well microplates, as used for the antibacterial assay was applied. The results were obtained after incubation of the microplate at temperatures ranging from 25°C to 37°C for 24 to 48 hours, depending on the specific candida strain.

### Antioxidant activity of REO

The DPPH solution were prepared based on the method of Molyneux and al.<sup>12</sup> with some modifications by solubilizing 2 mg of DPPH in 50 ml of 99% methanol, resulting in a precisely controlled concentration of approximately 4% (w/v). This solution was freshly prepared just before implementation to prevent the influence of light and oxidation. We also prepared a gradient of rosemary essential oil dilutions in methanol, spanning from 50 mg/ml to 1 mg/ml. Each dilution (0.2 ml) was meticulously mixed with 1.8 ml of the methanolic DPPH solution, ensuring thorough homogenization. Following a 30-minute incubation period at room temperature, shielded from light, we employed a UV-Vis spectrophotometer to determine the absorbance of each mixture at a specific wavelength of 515 nm. The calculation of inhibition percentages (I%) was based on a defined formula:

$$I\% = 100 \times ((A_{\text{blank}} - A_{\text{sample}}) / A_{\text{blank}})$$

A<sub>blank</sub>: Absorbance of the negative control

A<sub>sample</sub>: Absorbance in the presence of REO

These I% values offered valuable insights into the antioxidant effectiveness of *Rosmarinus officinalis* essential oil, with higher values signifying more potent antioxidant activity. Furthermore, we established the IC<sub>50</sub>, representing the concentration causing a 50% inhibition of DPPH radical activity, through dose-response curve analysis.

### Preparation of the Alginate/Chitosan and Chitosan crosslinked with TPP nanoparticles

#### a. Alginate/Chitosan nanoparticles

Two formulations were developed using a modified approach based on Natrajan and al.'s method<sup>13</sup> for encapsulating *Rosmarinus officinalis* essential oil within alginate and chitosan based nanoparticles (AL-CH.NP-REO). The first formulation (Formulation 1) employed chitosan and alginate at concentrations of 0.6 mg/ml each. Sodium alginate (30 mg) was dissolved in 50 ml of distilled water, and chitosan (30 mg) in 50 ml of 1% acetic acid solution. These solutions underwent overnight agitation at 300 rpm. Tween 80 (0.25 g) was added to 25 ml of the sodium alginate solution (0.6 mg/ml) to facilitate emulsification. Also 100 microliters of rosemary essential oil were gently introduced drop by drop into this aqueous mixture. After stirring for 20 minutes at 500 rpm, 5 ml of CaCl<sub>2</sub> solution (0.67 mg/ml) was gradually incorporated, followed by 30 minutes of stirring at 500 rpm. The resulting emulsion was then combined with 5 ml of chitosan solution (0.6 mg/ml), followed by another stirring for 30 minutes at 500 rpm, resulting in nanoparticles. For the formulation 2 (0.3 mg/ml chitosan and 0.3 mg/ml alginate), we adapted the concentrations of the polymers with the same protocol to assess their effects on nanoparticle properties, including size, morphology, and stability. The nanoparticles suspensions were stored at 4°C. The pH of the formulations was maintained in the range of 4.5 – 5.

#### b. Chitosan crosslinked with TPP nanoparticles

Two formulations were developed to encapsulate rosemary essential oil using chitosan nanoparticles (CH.NP-REO) via the ionic gelation method. The first formulation (Formulation 3) employed chitosan and TPP at concentrations of 2 mg/ml and 0.004 mg/ml respectively, we followed a procedure adapted from Ahmadi and al.<sup>14</sup> with some modifications. Chitosan (0.1 g) was dissolved in 50 ml of a 1% acetic acid solution, and this solution underwent overnight agitation at 300 rpm. Tween 80 (0.2 g) was added to the chitosan solution and was kept under vigorous stirring for 20 minutes. Then, 100 µl of REO was gradually added drop by drop followed by stirring at 500 rpm for 60 minutes. A solution of TPP was separately prepared by dissolving 0.04 g of TPP in 10 ml of distilled water. TPP solution was added dropwise to the first phase, then we stir it at 500 rpm for 60 minutes. In the second formulation (Formulation 4), chitosan and TPP concentrations were adjusted to 4 mg/ml and 0.008 mg/ml, respectively, with the same procedure as the first formulation. The nanoparticles were stored at 4°C. The pH of the nanoparticles in each trial was adjusted to maintain it between 4 and 4.5. This variation aimed to explore the effects of different polymer concentrations on nanoparticle properties, including size, stability, encapsulation capacity, and release properties.

### Characterization of nanoparticles

AL-CH.NP-REO and CH.NP-REO were characterized using various advanced techniques. Dynamic Light Scattering (DLS) analysis, conducted with a NanoPartica SZ-100V2 Series Nanoparticle Analyzer (HORIBA, Japan), provided data on particle size distribution, zeta potential for surface charge characterization, and the polydispersity index (PDI) indicating particle size uniformity within the sample, these manipulations were repeated three time. Scanning Electron Microscopy (SEM) imaging, utilizing the FEI Quanta 650 FEG (USA), revealed detailed surface morphology. Nanoparticle suspensions were carefully deposited onto a carbon-coated surface and allowed to naturally evaporate. This process ensured the nanoparticles adhered uniformly to the substrate, enabling comprehensive examination of their surface characteristics. UV-Vis absorption spectra were recorded in the wavelength range of 250 to 400 nm using a Jenway 7305 spectrophotometer (Hong Kong). Fourier-Transform Infrared (FTIR) spectroscopy, employing an FTIR-8900 spectrometer (Shimadzu, Japan), measurements were taken with a 4 cm<sup>-1</sup> resolution, spanning the spectral range from 4000 to 400 cm<sup>-1</sup>.

### Determination of encapsulation efficiency

To determine the encapsulation efficiency (EE), we followed a methodology outlined by Natrajan and al.<sup>13</sup> with some modifications. The centrifugation was carried out at 4000 rpm for 30 minutes, ensuring effective separation. Following centrifugation, the supernatant, was meticulously removed. 2 mL of ethanol was added to the tube containing the supernatant, followed by thorough vortex agitation and an additional 10-minute centrifugation. Subsequently, the absorbance of the collected supernatant was measured using a UV-Vis spectrophotometer at a wavelength of 287 nm. Utilizing a previously established calibration curve represented by the equation  $y = 0.2464x + 0.2242$  (with an R<sup>2</sup> of 0.998) we extrapolated the obtained absorbance to determine the concentration of the non-encapsulated essential oil.

Using the following formula, we calculated the (EE) of the nanoparticles:

$$EE (\%) = [(Total\ amount\ of\ oil - Free\ oil) / Total\ amount\ of\ oil] \times 100$$

**In vitro release studies**

The in vitro release studies were conducted at different pH values, pH 2 (acetate buffer) and pH 6 (phosphate buffer saline), this method was based on a procedure conducted by Esmaili and Asgari<sup>15</sup> with some modifications. The essential oil-loaded nanoparticles were separated from the aqueous suspension (750 µL) through centrifugation at 10,000 rpm for 10 minutes at 25°C. These isolated nanoparticles were then re-suspended in a buffer solution and gently agitated at 25°C. At specific time intervals, samples were subjected to centrifugation at 10,000 rpm for 5 minutes at 25°C, and the supernatant was collected and then mixed with ethanol (3 mL) for subsequent analysis. The amount of released REO was determined using a UV-Vis spectrophotometer, measuring absorbance at a wavelength of 287 nm. The cumulative release percentage (CRP) of REO released by the nanoparticles was calculated using the provided equation:

$$CRP (\%) = \sum_{t=0}^t \frac{Amount\ of\ Released\ oil}{Total\ amount\ of\ oil} \times 100$$

**In vivo analgesic activity**

Mice were fasted for 18 hours before the test, they were later treated as follow:

Group 1 received AL-CH.NP-REO (600 mg/kg of REO) orally. Group 2 received CH.NP-REO (800 mg/kg) orally. Group 3 received diluted essential oil (1000 mg/kg) in a suspension of physiological saline and Tween 80 orally. Group 4 received physiological saline orally, serving as the negative control. After 30 min, each mice received an injection of 0.0125 ml of 1% carrageenan subcutaneously under the plantar pad of the right hind paw. We start to measure the analgesic effect, two hours post-carrageenan injection. We utilized an Algesimeter (from Ugo Basile, Italy), an instrument for quantifying pain sensitivity in animals, to evaluate analgesic activity. This apparatus applied progressive force to the mice's paws using weights, starting with an initial weight. Additional weights of 250 gram were incrementally added to increase the force applied to the paw. When mice exhibited signs of pain, such as vocalization or agitation, the paw was immediately removed from the apparatus. The Algesimeter provided a quantitative measure of the force applied to induce a pain response in the inflamed paw. A higher measured force indicated a reduced sensitivity to pain, indicative of analgesic effects. To quantify the analgesic effect, we compared the test group mice to the negative control group that received carrageenan alone.

We calculated the percentage of analgesia using the formula:

$$Analgesia (\%) = [(FPT - FPC)/FPC] \times 100$$

FPT: Force applied to the test group paw FPC: Force applied to the control group paw

**RESULTS**

**Antibacterial activity of REO**

Concerning the antibacterial test, the results, were detailed in the graph above (Figure 1) that represent the variation in inhibition zone sizes for different treatments. Notably, treatment with REO 50 µl, REO 100 µl, and the positive control Gentamicin 10 mg.

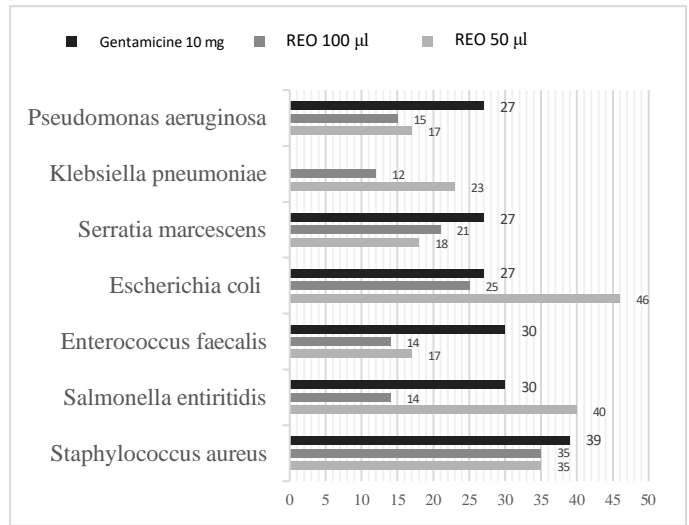


**Figure 1: Diameter of inhibition zones (mm) demonstrating antibacterial activity**

\* The diameter of the 6 mm blank disc and the 8 mm well is included in the zone of inhibition

**Determination of minimum inhibitory concentration (MIC) for Antibacterial activity**

The results of the minimum inhibitory concentration values for the bacterial strains in response to REO are presented in table 1. These MIC values offer insights into the sensitivity of each strain to REO.

**Table 1: Result of the antibacterial MIC**

Bacteria	Strain	MIC (µg /ml)
Staphylococcus aureus	ATCC 25923	0,008
Salmonella entiritidis	Pathogenic	4
Enterococcus faecalis	ATCC 29212	0,031
Escherichia coli	ATCC 25922	2
Serratia marcescens	Pathogenic	2
Klebsiella pneumoniae	Pathogenic	4
Pseudomonas aeruginosa	ATCC 27853	> 4

**Antifungal activity of REO**

The results obtained from both methods, namely the well diffusion agar and the disk diffusion agar, revealed significant inhibition diameters against the tested fungal strains that can be found in table 2.

**Table 2: Diameter of inhibition zones (mm) demonstrating antifungal activity**

Treatment	C.albicans	C.glabrata	C.kefyr
REO 50 µl	27 mm	23 mm	32 mm
REO 100 µl	40 mm	42 mm	70 mm

\* The diameter of the 6 mm blank disc and the 8 mm well is included in the zone of inhibition

### Determination of minimum inhibitory concentration (MIC) for Antifungal activity

The minimum inhibitory concentration (MIC) values for rosemary essential oil against various fungal strains are presented in table 3.

**Table 3: Result of the antifungal MIC**

Fungi	Strain	MIC ( $\mu\text{g/ml}$ )
<i>Candida albicans</i>	ATCC 25923	0,008
<i>Candida glabrata</i>	Pathogenic	4
<i>Candida kefyr</i>	ATCC 29212	4

### Antioxidant activity of REO

The results obtained regarding the inhibition percentage (1%) of different dilutions of rosemary essential oil (EO) with DPPH have been graphically represented in the following figures as a

**Table 4: DLS results for nanoparticle characteristics: Particle Size, Zeta Potential, and PDI**

Formulation	Particle size (nm)	Zeta potential (mv)	Polydispersity index
Formulation 1	83.33	-24	0.456
Formulation 2	50.53	-28	0.656
Formulation 3	57.09	+12	0.454
Formulation 4	72.87	+12.9	5.571

### Encapsulation efficiency

The (EE) was determined using an UV-Vis spectrophotometer at a wavelength of 287 nm. Utilizing a previously established calibration curve represented by the equation:

$y = 0.2464x + 0.2242$  (with an  $R^2$  of 0.998), the results are shown in the table 5.

*In vitro* release profiles of REO from CH.NP- REO and AL-CH.NP-

function of concentrations. The calculation method for inhibition percentages was applied as previously described, with the absorbance of the blank evaluated at 1.296 nm. From the curve of the antioxidant activity inhibition percentage as figured in figure 2 and the associated equation:  $y = 1.174x + 15.613$  (with an  $R^2 = 0.9603$ ), we determined the 50% inhibition concentration (IC<sub>50</sub>), which was found to be 29.29 mg/ml.

### Physicochemical characterization of CH.NP- REO and AL-CH.NP-REO

The utilization of Dynamic Light Scattering (DLS) analysis across the four distinct formulations allowed us to discern noteworthy variations in nanoparticle size. To provide a comprehensive overview of the formulation characteristics, a detailed summary is presented in Table 1. This table illustrates the mean nanoparticle sizes but also the polydispersity index and the potential zeta values.

### REO

After 4 hours, significant variations in cumulative release percentages were observed for each formulation and pH condition. At pH 2, all formulations exhibited low release of rosemary essential oil (REO). In contrast, at pH 6, there was an initial burst release of oil observed for all formulations. These findings are visually represented in Figure 5.

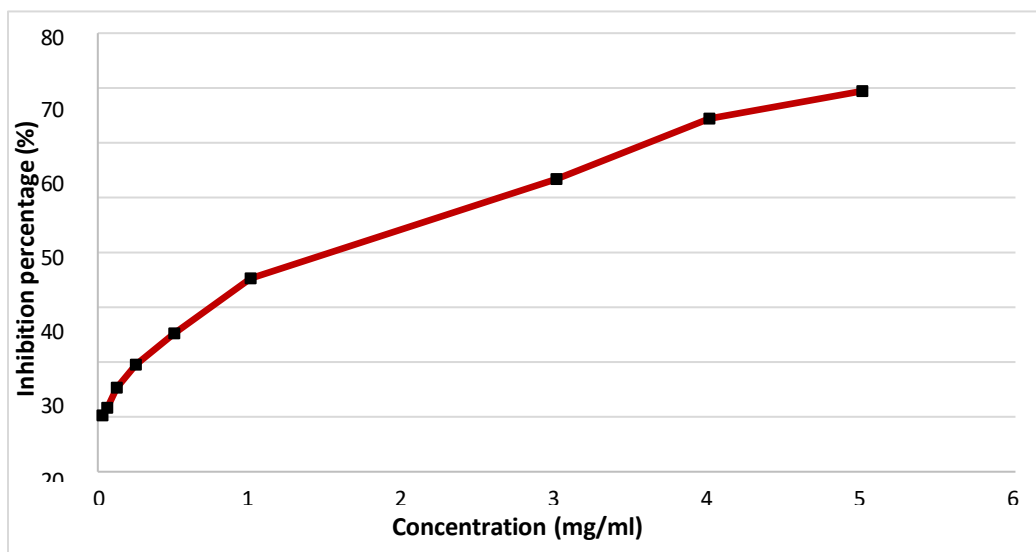


**Figure 2: Percentage Inhibition curve of the antioxidant activity of rosemary essential oil**

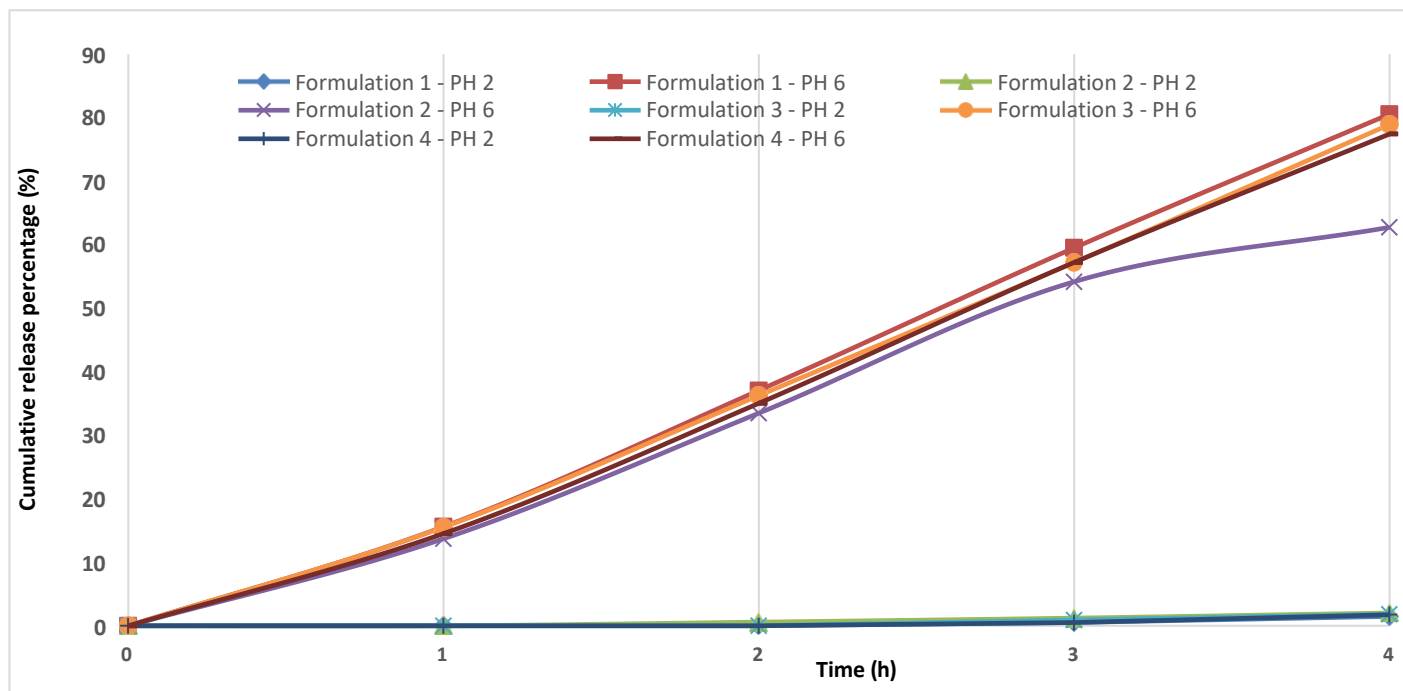


**Figure 3: In vitro release profile of nanoparticles at pH 2 and pH 6**

#### FT-IR analysis

Our study conducted Fourier Transform Infrared analysis on several key components, including Rosmarinus essential oil (REO), chitosan nanoparticles encapsulating REO, blank chitosan nanoparticles, alginate/chitosan nanoparticles encapsulating REO, and blank alginate/chitosan nanoparticles. In our FTIR analysis of rosemary essential oil as shown in figure, distinct peaks indicated the presence of key functional groups: O-H stretching ( $3452\text{ cm}^{-1}$ ) for hydroxyl groups, C-H stretching ( $2950\text{ cm}^{-1}$ ) for alkyl groups, and C=O stretching ( $1743\text{ cm}^{-1}$ ) for carbonyl compounds. We also observed a C=C stretching peak ( $1635\text{ cm}^{-1}$ ) for unsaturated compounds and minor peaks for alkyl groups ( $1458\text{ cm}^{-1}$  and  $1369\text{ cm}^{-1}$ ).

The analysis of the blank chitosan nanoparticles, and chitosan nanoparticles encapsulating rosemary essential oil, revealed several significant functional groups and interactions. At  $3402\text{ cm}^{-1}$ , stretching vibrations of hydroxyl (-OH) groups were detected, indicating the presence of alcohol or phenolic compounds. The peak at  $3317\text{ cm}^{-1}$  suggested N-H stretching vibrations, which are typically associated with amines or amides. The peak at  $1639\text{ cm}^{-1}$  corresponds to C=C stretching

vibrations, commonly found in compounds with double bonds like alkenes or aromatic rings. Similarly, the peak at  $1515\text{ cm}^{-1}$  is indicative of C=C stretching vibrations in aromatic compounds. At  $1087\text{ cm}^{-1}$ , the C-O stretching vibrations were observed, pointing towards the presence of alcohols, ethers, or esters. Finally, the peak at  $547\text{ cm}^{-1}$  may suggest bending vibrations of halogenated compounds.

Several key functional groups were identified in the FTIR specters of the blank alginate/chitosan nanoparticles, and alginate/chitosan nanoparticles encapsulating rosemary essential oil as figured in the graph. At  $3502\text{ cm}^{-1}$ , a strong peak indicated the presence of hydroxyl (OH) groups, which are commonly associated with alcohols and phenols.

The shift to  $3407\text{ cm}^{-1}$  in some samples suggested weak interactions between hydroxyl groups of the essential oil and those of the alginate/chitosan nanoparticles. A distinct peak at  $1742\text{ cm}^{-1}$  was observed, which is typically attributed to carbonyl (C=O) groups found in ketones and aldehydes. Additionally, a peak at  $1076\text{ cm}^{-1}$  hinted at the presence of ether or ester groups in the samples.

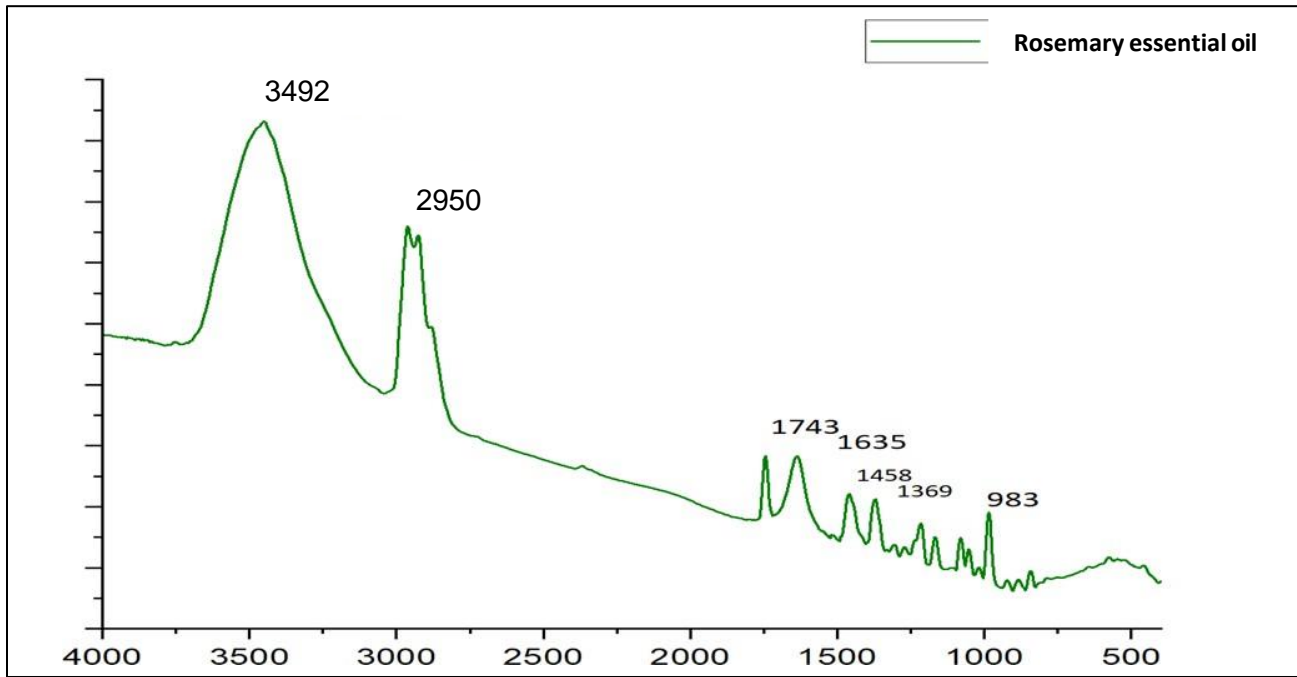


Figure 4: FTIR Spectrum of *Rosmarinus officinalis* essential oil

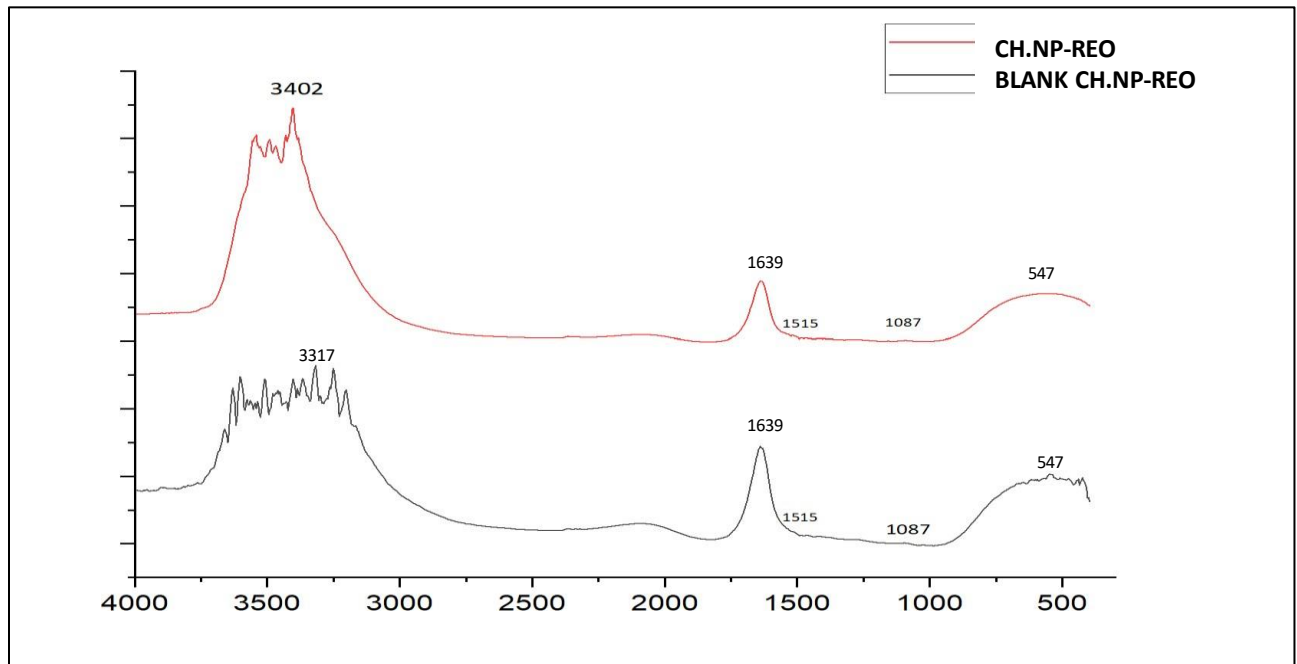
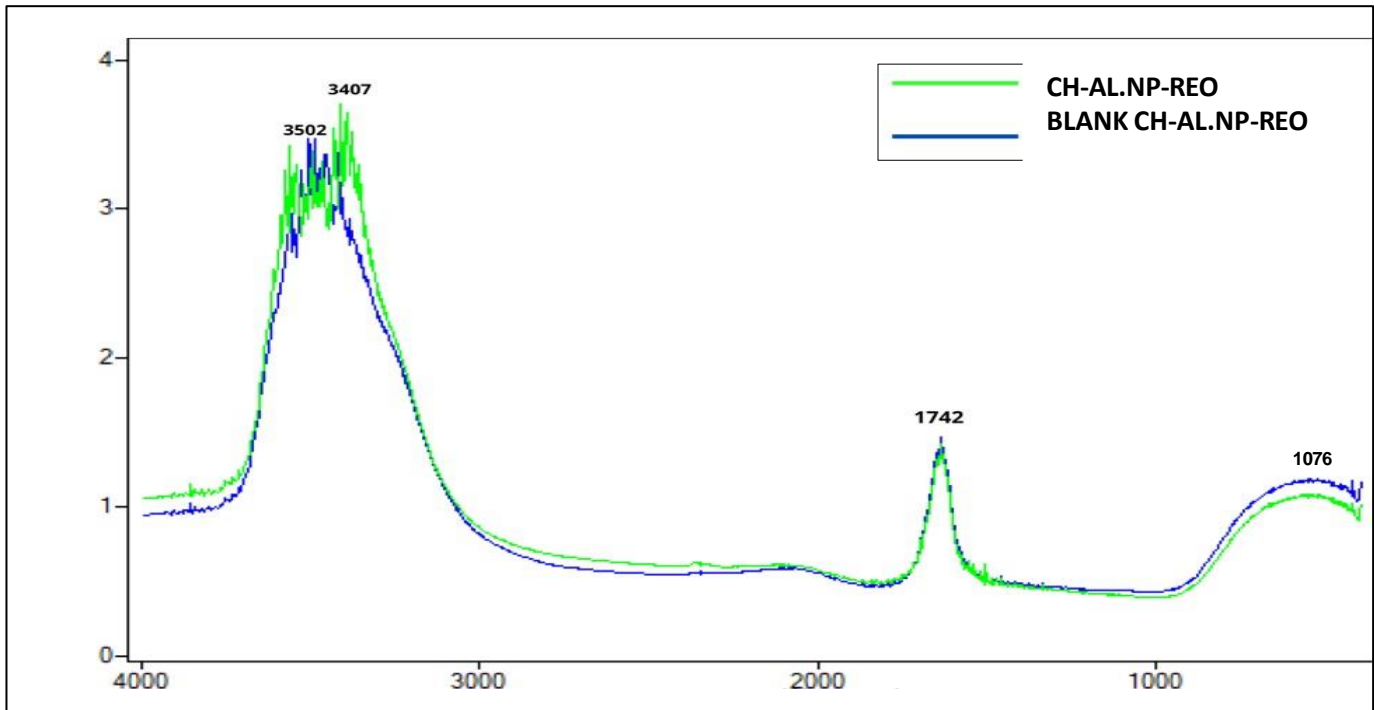


Figure 5: FTIR Spectrum of chitosan nanoparticles encapsulating REO and blank chitosan nanoparticles

### 3.5 Scanning electron microscopy

The results of scanning electron microscopy (SEM) are presented in the following figures. These images provide varying levels of detail on the studied nanoparticles, allowing for the observation of their morphology, and structure. High vacuum technique was employed for SEM sample observation, enabling higher resolution and improved visualization of NP details.

During the SEM observation of the nanoparticles, promising outcomes were obtained. Although the precise structure and shape of the nanoparticles were not distinctly discernible, their presence in the samples was observed. It is worth noting that the nanoparticles were in suspension before observation, which may pose a challenge when using SEM. Nonetheless, an agglomeration of different nanoparticles with a homogeneous structure was observed in both studied formulations.



**Figure 6: FTIR Spectrum of alginate/chitosan nanoparticles encapsulating REO and blank alginate/chitosan nanoparticles**

#### In vivo analgesic activity

Our study results reveal a dose-response relationship in the evaluated analgesic activity. Rosemary essential oil in group 1 demonstrated exceptional analgesic activity, with a high percentage of 76.65% pain reduction observed in mice. In the

case of group 2, with a concentration of 800 mg/kg, CH.NP-REO showed an analgesic activity percentage of 41.01%. However, in group 3, AL-CH.NP-REO encapsulating the essential oil, at a concentration of 600 mg/kg, exhibited the lowest percentage of analgesic activity, only 5%.

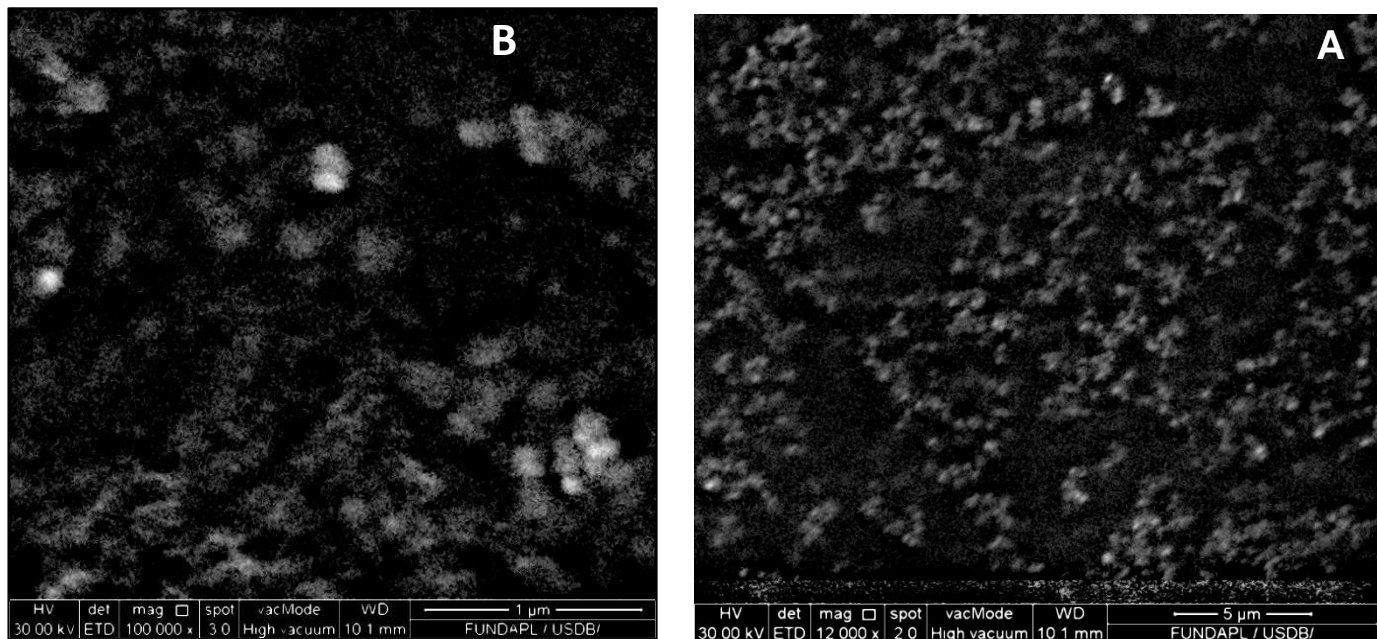


**Figure 7: Scanning electron microscopic images: (A) CH.NP-REO; (B) AL-CH.NP-REO**



## DISCUSSION

The evaluation of the antibacterial activity of rosemary essential oil (REO) demonstrated promising results using the inhibition zone diameters as indicators. The observed inhibition zones are highly significant, especially for strains such as *Staphylococcus aureus* ATCC 25923, pathogenic *Salmonella enteritidis*, *Escherichia coli* ATCC 25922, and pathogenic *Serratia marcescens*. These strains exhibited a high sensitivity to rosemary oil, indicating its potential as an effective antibacterial agent against these pathogenic microorganisms. These findings align with reports from other authors who demonstrated that rosemary oil has bactericidal effects on both Gram-positive and Gram-negative bacteria<sup>16</sup>. The antibacterial activity of rosemary oil can be attributed to its chemically rich composition of pinenes, camphor, and 1,8-cineole<sup>17</sup>. These compounds have synergistic effects that disrupt bacterial membranes and inhibit protein synthesis<sup>18</sup>. Discs impregnated with REO generated larger inhibition zones compared to oil-containing wells, suggesting broader diffusion of active compounds in the culture medium despite the lower concentration. A study conducted by Abolfazl Jafari Sales and al.<sup>19</sup>, reported different MIC values from those obtained in our study. They found the MIC of rosemary oil to be 1.25 µg/ml for *E. coli* and 0.625 µg/ml for *S. aureus*. While there is a slight difference between our results and those of Abolfazl Jafari Sales and al., it is suggested that there is some correlation between the two studies. In a prior study by Gauch and al.<sup>20</sup>, the antifungal activity of rosemary essential oil against *Candida albicans* was evaluated, and an inhibition diameter of 45 mm was reported. This alignment between their results and ours reinforces the credibility of rosemary essential oil's antifungal activity against *Candida albicans*. Rosemary essential oil contains various phytochemical compounds, such as camphor, cineol, flavonoids, and terpenes, which have demonstrated antifungal properties in various studies<sup>21</sup>. The antioxidant activity of rosemary oil is attributed to specific chemical compounds within it. A previous study conducted by Wang and al.<sup>22</sup> confirmed that rosemary essential oil contains compounds such as 1-8 cineole, alpha-pinene, and beta-pinene, which have exhibited significant antioxidant activity. These compounds can act as antioxidants by neutralizing free radicals and preventing oxidative damage. Obtaining an IC<sub>50</sub> of 29.29 mg/ml indicates that rosemary essential oil possesses considerable antioxidant activity. This suggests that this essential oil may have the potential to combat the harmful effects of free radicals and help prevent oxidative damage in a biological context. In formulation 1, the average nanoparticle size was relatively high compared to the other formulations. This is due to the relatively high concentrations of chitosan/alginate. High polymer concentrations can lead to larger nanoparticles, as observed by Guinebrière and al.<sup>23</sup>. It's possible that electrostatic interactions between chitosan and alginate increase nanoparticle stability and size. Conversely, formulation 2 showed a significant reduction in nanoparticle size, this size decrease can be attributed to the reduction in the amount of polymers in the nanoparticle matrix. The formulation 4 recorded a size slightly higher than the formulation 3. This can be explained by the fact that this formulation contains a higher chitosan concentration (4 mg/ml) than the third formulation (2 mg/ml). It's possible that the increased chitosan concentration leads to more electrostatic interactions with rosemary essential oil, thereby increasing nanoparticle size. A comparative analysis with Natrajan and al. results<sup>13</sup> reveals notable differences. Their first formulation with a concentration of alginate/chitosan nanoparticles (0.6 mg/ml - 0.6 mg/ml) yielded nanoparticle sizes of approximately 226 nm, considerably larger than our

result. They also formulated a second formulation with a concentration of alginate/chitosan nanoparticles (0.3 mg/ml - 0.3 mg/ml), obtaining a size of 59.34 nm, which is nearly identical to our measurement for the formulation 3, indicating a correlation between the results. Regarding the comparison with Ahmadi et al.'s results<sup>14</sup>, our formulation 3 and 4 exhibited smaller nanoparticle sizes than those obtained in their study (140 nm). The zeta potential results indicate good nanoparticle stability across all formulations. High positive or negative surface charges create electrostatic repulsion between particles, preventing aggregation. The presence of positive charges in chitosan-based nanoparticles can be attributed to the amine groups within chitosan's chemical structure<sup>24</sup>. The results obtained concerning formulation 1 and 2 are consistent with the research by Keawchoon and al.<sup>25</sup>, which reported negative zeta potential values between -19 mV and -23 mV, in line with our own findings. Our polydispersity index (PDI) results are notably consistent with those obtained by Cai and al.<sup>26</sup> comparing to formulations 1,2 and 3, the values obtained are closely align with those reported by Cai et al. who obtained PDI values ranging from 0.222 to 0.425. A low PDI suggests a uniform particle size distribution, essential for ensuring stability and optimal efficiency in controlled release systems. However, formulation 4 exhibits a significantly higher PDI of 5.571. This elevated value implies an extensive and heterogeneous distribution of particle sizes. It likely reflects substantial variability in nanoparticle sizes, with the presence of vastly different-sized particles within this formulation. Concerning the results of encapsulation efficiency, in formulation 1, we achieved an encapsulation rate of 98.04%. which is substantially higher than that reported in a similar study by Natrajan and al.<sup>13</sup> obtaining a rate of 86.9%. Despite alterations in polymer concentrations, formulation 2 maintained a high encapsulation capacity, and the results are consistent with those of formulation 1. Formulation 3 attained an encapsulation rate of 99.03%, in line with the findings of a prior study conducted by Ahmadi and al.<sup>14</sup> whereas they obtained an encapsulation rate of 92.49% for their formulation. These results confirm the effectiveness of our methodology in encapsulating rosemary essential oil within chitosan nanoparticles, demonstrating notable reproducibility. For formulation 4, we achieved a slight but significant improvement compared to the first formulation. This enhancement suggests that increasing the chitosan concentration and decreasing the volume of rosemary essential oil may have a positive impact on encapsulation efficiency, highlighting the flexibility of our method. Regarding the limited oil release by nanoparticles in all four formulations at pH 2, it may be attributed to the positively charged protonated amino groups on chitosan, promoting essential oil interaction and retention within the nanoparticles<sup>15</sup>. This enhanced retention could also result from electrostatic interactions between chitosan's positive groups and essential oil components, and with the carboxylate groups of alginate in the case of formulations 1 and 2, potentially reinforcing nanoparticle structure, thus preventing significant oil release. Another theory suggests that in an acidic environment rich in H<sup>+</sup> ions (protons), the protonated amine groups of chitosan may interact with H<sup>+</sup> ions through ionic interactions, strengthening particle interactions and potentially reducing essential oil release. At pH 6, the initial burst release of oil in all four formulations is due to oil molecules adsorbed on the particle's surface, trapped near the surface. When nanoparticles encounter the dissolution medium, the high dissolution rate of the polymer near the surface leads to the rapid release of these adsorbed oil molecules, resulting in the observed burst release phenomenon<sup>27</sup>. In a slightly alkaline solution, the deprotonation

of chitosan amine groups alters the charge balance, weakening ionic interactions, and potentially leading to particle destabilization or disintegration. This weakens the ionic interactions between cationic chitosan and anions present in the environment, including TPP, resulting in essential oil release<sup>15</sup>. The analgesic activity of rosemary essential oil is attributed to its active compounds, such as camphor and 1,8-cineole, which have demonstrated analgesic properties, as demonstrated by Raskovic and al. in a previous study<sup>28</sup>. In our research discussions, a clear dose-response pattern emerges from our findings. The percentage of analgesic activity obtained concerning the nanoparticles encapsulating essential oil, suggests that the nanoparticles have effectively encapsulated the rosemary essential oil, allowing for a controlled and extended release of its active components. These findings provide encouraging evidence supporting the potential of nanoparticles as a delivery system for therapeutic compounds, including essential oils.

## CONCLUSION

The study conducted on the encapsulation of *Rosmarinus officinalis* essential oil (REO) within CH.NP-REO and AL-CH.NP-REO represents a fascinating and promising endeavor. REO exhibited remarkable efficacy as an antibacterial agent, notably against strains of *Staphylococcus aureus* and *Salmonella*, known for their involvement in common infections. Furthermore, its antifungal activity against *Candida* strains, including *Candida albicans*, was substantial. The antioxidant activity of REO was also confirmed through the DPPH free radical assay, with a GI50 of 29.29 mg/ml, signifying a strong capacity to neutralize free radicals and protect against oxidative damage. The successful formulation of nanoparticles encapsulating rosemary essential oil was achieved, highlighting our ability to create well-defined and effective particles. DLS results revealed particle sizes below 100 nm, indicating our success in formulating nanoscale nanoparticles. Additionally, zeta potential analysis demonstrated good particle stability. While the polydispersity index highlighted the homogeneity of most formulations, except for formulation 4, which exhibited significant heterogeneity. The use of FTIR allowed us to determine chemical interactions and compounds within the nanoparticles, further reinforcing the success of the formulation. Through UV-Vis spectroscopy, we assessed the efficiency of REO encapsulation within the formulated nanoparticles. The results confirmed the perfect encapsulation of REO, with an encapsulation rate exceeding 98% in most formulations. This effective encapsulation ensures the stability and preservation of REO properties. Furthermore, the in vitro release profile demonstrated that the nanoparticles would withstand the gastric environment and release the essential oil in the small intestine for optimal absorption. In vivo evaluation of analgesic activity, conducted on mice following oral administration of nanoparticles encapsulating essential oil, revealed intriguing and even impressive results. The evaluation of analgesic activity revealed a dose-response relationship, with excellent results, notably the case of the CH.NP-REO. This study represents only a first step toward further exploration of the potential applications of these nanoparticles. There is still much work to be done to optimize formulations, study their stability, biodisponibility and pharmacological activity in vivo and in vitro. We hope to continue our research in this exciting field, advancing further scientific breakthroughs. These nanoparticles offer promising prospects for the development of more effective and targeted medications, thus opening new opportunities in the field of pharmacy and medicine.

## REFERENCES

- Malshe A. Nanotechnology. In: Chatti S, Laperrière L, Reinhart G, Tolio T, editors. CIRP Encyclopedia of Production Engineering. Berlin, Heidelberg: Springer Berlin Heidelberg; 2019.p.1260-7. doi: [https://doi.org/10.1007/978-3-662-53120-4\\_16731](https://doi.org/10.1007/978-3-662-53120-4_16731)
- Severino P, da Silva CF, Andrade LN, de Lima Oliveira D, Campos J, Souto EB. Alginate nanoparticles for drug delivery and targeting. *Current pharmaceutical design*, 2019;25(11):1312-34. doi: <http://doi.org/10.2174/1381612825666190425163424>
- Kadam RS, Bourne DW, Kompella UB. Nano-advantage in enhanced drug delivery with biodegradable nanoparticles: contribution of reduced clearance. *Drug Metabolism and Disposition*, 2012;40(7):1380-8. doi: <https://doi.org/10.1124/dmd.112.044925>
- Andrade JM, Faustino C, Garcia C, Ladeiras D, Reis CP, Rijo P. *Rosmarinus officinalis* L.: an update review of its phytochemistry and biological activity. *Future science OA*, 2018;4(4):FSO283. doi: <https://doi.org/10.4155/fsoa-2017-0124>
- Borges RS, Ortiz BLS, Pereira ACM, Keita H, Carvalho JCT. *Rosmarinus officinalis* essential oil: A review of its phytochemistry, anti-inflammatory activity, and mechanisms of action involved. *Journal of ethnopharmacology*, 2019;229(29-45). doi: <https://doi.org/10.1016/j.jep.2018.09.038>
- Delshadi R, Bahrami A, Tafti AG, Barba FJ, Williams LL. Micro and nano-encapsulation of vegetable and essential oils to develop functional food products with improved nutritional profiles. *Trends in Food Science & Technology*, 2020;104(72-83). doi: <https://doi.org/10.1016/j.tifs.2020.07.004>
- Patra JK, Das G, Fraceto LF, Campos EVR, Rodriguez-Torres Mdp, Acosta-Torres LS, et al. Nano based drug delivery systems: recent developments and future prospects. *Journal of Nanobiotechnology*, 2018;16(1):71. doi: <http://doi.org/10.1186/s12951-018-0392-8>
- Magaldi S, Mata-Essayag S, De Capriles CH, Pérez C, Colella M, Olaizola C, Ontiveros Y. Well diffusion for antifungal susceptibility testing. *International journal of infectious diseases*, 2004;8(1):39-45. doi: <https://doi.org/10.1016/j.ijid.2003.03.002>
- Nathan P, Law EJ, Murphy DF, MacMillan BG. A laboratory method for selection of topical antimicrobial agents to treat infected burn wounds. *Burns*, 1978;4(3):177-87. doi: [https://doi.org/10.1016/S0305-4179\(78\)80006-0](https://doi.org/10.1016/S0305-4179(78)80006-0)
- Aouni M, Pelen F, Soulimani R. Étude de l'activité antimicrobienne d'un mélange de 41 huiles essentielles et domaines d'application. *Phytothérapie*, 2013;11(4):225-36. doi: <https://doi.org/10.1007/s10298-013-0790-x>
- Kowalska-Krochmal B, Dudek-Wicher R. The minimum inhibitory concentration of antibiotics: Methods, interpretation, clinical relevance. *Pathogens*, 2021;10(2):165. doi: <https://doi.org/10.3390/pathogens10020165>
- Molyneux P. The use of the stable free radical diphenylpicrylhydrazyl (DPPH) for estimating antioxidant activity. *Songklanakarin J sci technol*, 2004;26(2):211-9.
- Natrajan D, Srinivasan S, Sundar K, Ravindran A. Formulation of essential oil-loaded chitosan-alginate nanocapsules. *Journal of food and drug analysis*, 2015;23(3):560-8. doi: <https://doi.org/10.1016/j.jfda.2015.01.001>
- Ahmadi Z, Saber M, Bagheri M, Mahdavinia GR. Achillea millefolium essential oil and chitosan nanocapsules with enhanced activity against *Tetranychus urticae*. *Journal of pest science*, 2018;91(837-48). doi: <https://doi.org/10.1007/s10340-017-0912-6>
- Esmaili A, Asgari A. In vitro release and biological activities of *Carum copticum* essential oil (CEO) loaded chitosan nanoparticles. *Int J Biol Macromol*, 2015;81(283-90). doi: <http://doi.org/10.1016/j.ijbiomac.2015.08.010>
- Stojiljkovic J, Trajchev M, Nakov D, Petrovska M. Antibacterial

activities of rosemary essential oils and their components against pathogenic bacteria. *Advances in Cytology & Pathology*, 2018. doi: <https://doi.org/10.15406/acp.2018.03.00060>

17. Bajalan I, Rouzbahani R, Pirbalouti AG, Maggi F. Antioxidant and antibacterial activities of the essential oils obtained from seven Iranian populations of *Rosmarinus officinalis*. *Industrial Crops and Products*, 2017;107(305-11).doi: <https://doi.org/10.1016/j.indcrop.2017.05.063>

18. Burt S. Essential oils: their antibacterial properties and potential applications in foods--a review. *Int J Food Microbiol*, 2004;94(3):223-53. doi: 10.1016/j.ijfoodmicro.2004.03.022. doi: <https://doi.org/10.1016/j.ijfoodmicro.2004.03.022>

19. JAFARI-SALES A, Pashazadeh M. Study of chemical composition and antimicrobial properties of Rosemary (*Rosmarinus officinalis*) essential oil on *Staphylococcus aureus* and *Escherichia coli* in vitro. *International Journal of Life Sciences and Biotechnology*, 2020;3(1):62-9. doi: <https://doi.org/10.38001/ijlsb.693371>

20. Gauch LMR, Pedrosa SS, Esteves RA, Silveira-Gomes F, Gurgel ESC, Arruda AC, Marques-da-Silva SH. Atividade antifúngica de *Rosmarinus officinalis* Linn. óleo essencial contra *Candida albicans*, *Candida dubliniensis*, *Candida parapsilosis* e *Candida krusei*. *Revista Pan-Amazônica de Saúde*, 2014;5(1):61-6. doi: <https://doi.org/10.5123/S2176-62232014000100007>

21. Özcan MM, Chalchat J-C. Chemical composition and antifungal activity of rosemary (*Rosmarinus officinalis* L.) oil from Turkey. *International journal of food sciences and nutrition*, 2008;59(7-8):691-8. doi: <https://doi.org/10.1080/09637480701777944>

22. Wang W, Wu N, Zu YG, Fu YJ. Antioxidative activity of *Rosmarinus officinalis* L. essential oil compared to its main components. *Food Chemistry*, 2008;108(3):1019-22. doi:

<https://doi.org/10.1016/j.foodchem.2007.11.046>

23. Guinebretière S, Briançon S, Fessi H, Teodorescu VS, Blanchin MG. Nanocapsules of biodegradable polymers: preparation and characterization by direct high resolution electron microscopy. *Materials Science and Engineering: C*, 2002;21(1):137-42. doi: [https://doi.org/10.1016/S0928-4931\(02\)00073-5](https://doi.org/10.1016/S0928-4931(02)00073-5)

24. Matshetshe KI, Parani S, Manki SM, Oluwafemi OS. Preparation, characterization and in vitro release study of  $\beta$ -cyclodextrin/chitosan nanoparticles loaded Cinnamomum zeylanicum essential oil. *Int J Biol Macromol*, 2018;118(Pt A):676-82. doi: [10.1016/j.ijbiomac.2018.06.125](https://doi.org/10.1016/j.ijbiomac.2018.06.125)

25. Keawchaoon L, Yoksan R. Preparation, characterization and in vitro release study of carvacrol-loaded chitosan nanoparticles. *Colloids and surfaces B: Biointerfaces*, 2011;84(1):163-71. doi: <https://doi.org/10.1016/j.colsurfb.2010.12.031>

26. Cai M, Wang Y, Wang R, Li M, Zhang W, Yu J, Hua R. Antibacterial and antibiofilm activities of chitosan nanoparticles loaded with *Ocimum basilicum* L. essential oil. *International Journal of Biological Macromolecules*, 2022;202(122-9). doi: <https://doi.org/10.1016/j.ijbiomac.2022.01.066>

27. Anitha A, Deepagan V, Rani VD, Menon D, Nair S, Jayakumar R. Preparation, characterization, in vitro drug release and biological studies of curcumin loaded dextran sulphate-chitosan nanoparticles. *Carbohydrate Polymers*, 2011;84(3):1158-64. doi: <https://doi.org/10.1016/j.carbpol.2011.01.005>

28. Raskovic A, Milanovic I, Pavlovic N, Milijasevic B, Ubavic M, Mikov M. Analgesic effects of rosemary essential oil and its interactions with codeine and paracetamol in mice. *Eur Rev Med Pharmacol Sci*, 2015;19(1):165-72.